Mech. Engg.Res. Bull
Vol.13 (1990) pp 15-26

Prediction of the Gas Flow and Concentration of Fresh Charge Iin the Cylinder of A Two-stroke Cycle Uniflow Engine During Scavenging

Md. Imtiaz Hossain*

ABSTRACT

The quasi three-dimensional DICE** code is modified to predict gas flow and the concentration of fresh charge in the cylinder of a two-cycle uniflow scavenged diesel engine. The modified code incorporates the geometry of the relevant cylinder and the port assemblies as well as the physical conditions of operation. The flow is assumed axi-symmetric. The inlet ports are simulated as an annular openning in the liner. The exhaust port is simulated as a central hole in the cylinder head and a valve with a given motion is maintained there to describe the openning and closing of the exhaust port. The mathematical model consists of seven dependent transport equations in the quasi three-dimensional form. These equations are then transformed into a form so as to allow the domain of solution to be confined in the volume occupied by the gas and also fit the geometry of the cylinder ports. The transformed equations are solved numerically employing the finite difference techniques. Results are presented in the form of mean velocity field, turbulent kinetic energy distribution and gas concentration distribution inside the cylinder.

INTRODUCTION

Investigations directed to identify the causes of the unwanted features of the 2-cycle engines reveal that the performance of the two-cycle engines depends largely on the effectiveness of scavenging the cylinder. Thus the scavenging process of the two-stroke cycle engines deserve proper attention because except for its unacceptable fuel consumption and undesirable emission the two stroke cycle engine is a very lucrative prime mover.

The scavenging process in the two-cycle engines are considerably different from that in the four-cycle engines. In this paper, the flow-structure prevailing inside the cylinder during the gas-exchange process in a uniflow two-cycle engine is closely examined so far as the gas-motion and its composition is concerned.

Studies reported in Mirko et al (1985), Sanborn et al (1985), Sweeny (1985), Sher (1982) and Ekchian (1979) give an account of the flow visualisation studies on the scavenging process in given engine cylinders. The information about the in-cylinder flow-fields are, therefore, of the qualitative nature. Experimental measurements reported in Snauwaert et al (1986), Vafidis et al (1986), Nishimoto et al (1984), Sung et al (1982), Tindal et al (1974) and Ohigashi (1960) provide some quantitative information on the effects of various parameters like 'Inlet Port Angle', 'Flow Reynolds Number', 'Exhaust Geometry', 'Swirl' etc. on the in-cylinder flow-field mostly under steady-state conditions of operation but there is little information on the composition of the gas in the cylinder. Investigations by Diwakar (1987), Wakisaka et al (1986), Yamada et al (1986), Amsden et al (1985), Diwakar (1985), Verhoebe (1985) provide multi-dimensional computer models for assessing the in-cylinder flow structure in further detail but again information on the in-cylinder gas composition and the manner in which the gas composition varies with time as scavenging proceeds is absent.

Assumptions:

In order to predict and analyse the fluid motion in the cylinder of a simulated two-stroke cycle engine the following main assumptions have been made.

i. Both the fresh charge and the products of combustion obey the ideal gas and the Newtonian viscosity laws and they have properties same as that of air.

ii. The cylinder wall temperature may be regarded

* Department of Mechanical Engineering, BUET, Dhaka, Bangladesh.

as being steady.

iii. The in-cylinder processes can be adequately described by their statistically averaged properties and hence the conservation of mass, momentum and energy equations may be solved in their ensemble averaged form.

iv. The information about the turbulence structure and its effect on the mean flow can be provided by the K-ε model.

v. The turbulent Prandtl/Schmidt number may be assigned a constant value of order unity.

vi. The inlet ports on the cylinder may be considered as a slit on the circumference.

vii. The system may be reduced to a two-dimensional problem by utilizing the symmetrical geometry of the cylinder and port assembly with respect to a plane which contains the cylinder axis.

viii. A uniform velocity profile is assumed at the inlet and exhaust ports and no back-flow is allowed.

ix. The instantaneous composition of the exhaust gas is equal to the local gas composition at a point adjacent to the exhaust port.

MATHEMATICAL MODEL

Under the above assumptions the flow-field inside the cylinder was determined by the solution of seven dependent transport equations, namely: the conservation of total mass, the conservation of the mass of fresh charge, the conservation of axial momentum, the conservation of radial momentum, the conservation of energy, the transport equation for turbulent kinetic energy and the equation for the rate of dissipation of turbulent kinetic energy.

These may be completely represented by a general transport equation of the form:

$$\frac{\partial}{\partial t}(\rho\phi) + \operatorname{div}(\rho u \phi) = \operatorname{div}\left(\Gamma_{\phi} \operatorname{grad} \phi\right) + S_{\phi}$$

For a particular dependent variable ϕ, the appropriate meaning of the diffusion coefficient Γ_ϕ and the source term S_ϕ are summerised in Table 1. The values of the turbulence model constants are provided in Table 2.

Table 1

Conservation of	Variable ϕ	Γ_ϕ	S_ϕ
Total mass	1	0	0
Mass of Fresh charge	x	$D_{AB,t}$	0
Axial momentum	U_z	μ_t	Pressure gradient in direction + other sources
Radial Momentum	U_r	μ_t	Pressure gradient in direction + other sources
Total energy	h	μ_t/σ_h	$-\partial p/\partial t$
Turbulence Kinetic energy	K	μ_t/σ_k	$G-\rho\varepsilon$
Dissipation rate of turbulence K.E.	ε	μ_t/σ_ε	$C_1 G\varepsilon/K - C_2\rho\varepsilon^2/K + \rho\varepsilon\nabla.\overline{U}$

The gird structure adopted for the analysis is shown in figure 1. It consists of arbitrarily spaced planes of constant r and z. All the scalar quantities including angular velocity, enthalpy, density and viscosity are calculated at the nodal points of the grid. The velocities are located at the mid-position between the pressures which drive them. For unsteady (moving piston) calculations a grid structure of mesh size 34 X 34 was employed.

Table 2

Turbulence model Constant	Value
C_1	1.44
C_2	1.92
K	0.4187

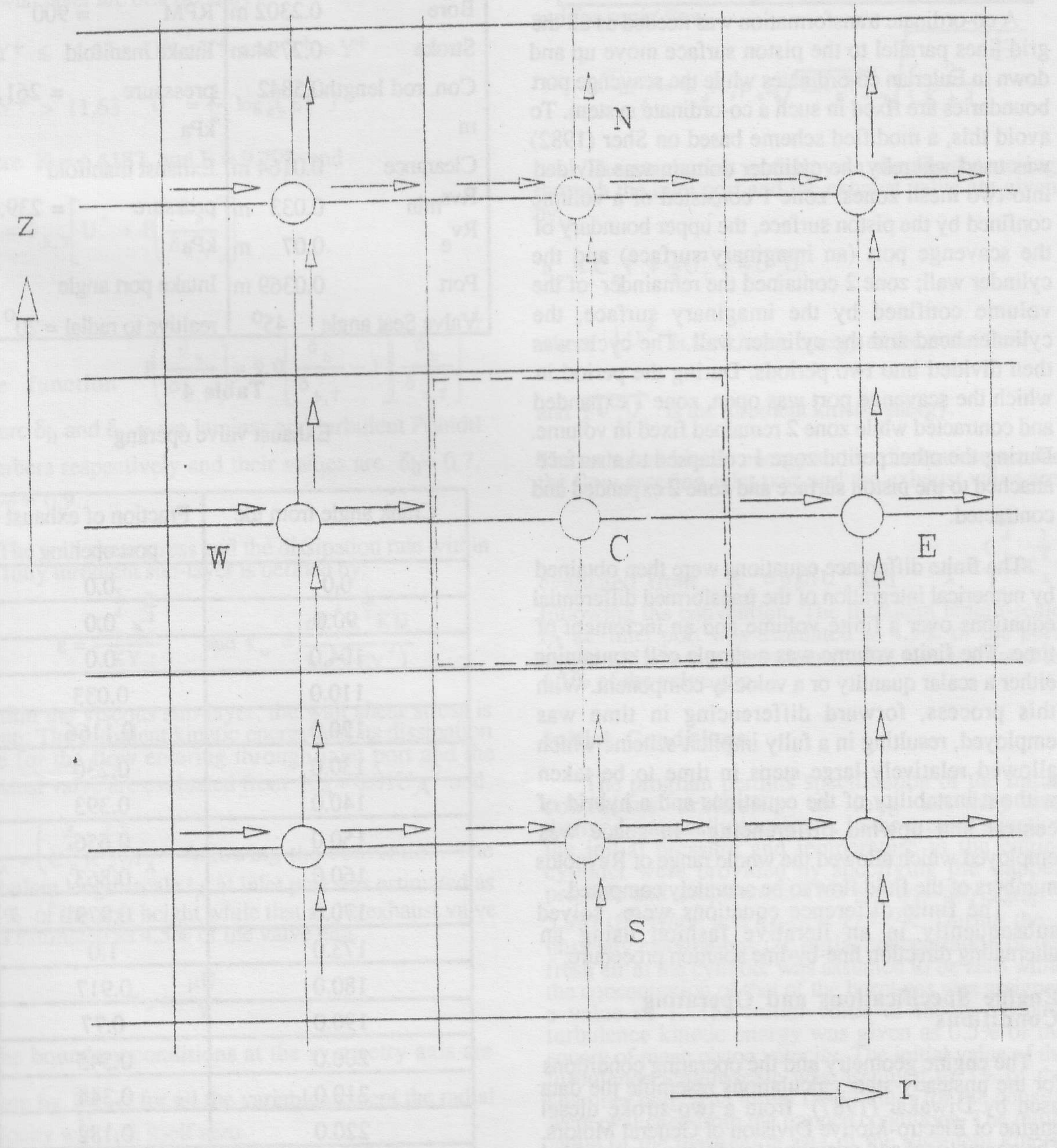

Figure 1 : The Grid structures.

E	9.793
σ_h	0.9
σ_K	1.0
σ_ε	-1.22

A co-ordinate transformation was needed as all the grid lines parallel to the piston surface move up and down in Eulerian co-ordinates while the scavenge port boundaries are fixed in such a co-ordinate system. To avoid this, a modified scheme based on Sher (1982) was used whereby the cylinder domain was divided into two mesh zones: zone 1 consisted of a volume confined by the piston surface, the upper boundary of the scavenge port (an imaginary surface) and the cylinder wall; zone 2 contained the remainder of the volume confined by the imaginary surface, the cylinder head and the cylinder wall. The cycle was then divided into two periods. During the period in which the scavenge port was open, zone 1 expanded and contracted while zone 2 remained fixed in volume. During the other period zone 1 collapsed to a surface attached to the piston surface and zone 2 expanded and contracted.

The finite difference equations were then obtained by numerical integration of the transformed differential equations over a finite volume and an increment of time. The finite volume was a simple cell containing either a scalar quantity or a velocity component. With this process, forward differencing in time was employed, resulting in a fully implicit scheme which allowed relatively large steps in time to be taken without instability of the equations and a hybrid of central and upwind differencing in space was employed which allowed the whole range of Reynolds numbers of the fluid flow to be acurately computed.

The finite difference equations were solved subsequently in an iterative fashion using an alternating direction line-by-line solution procedure.

Engine Specifications and Operating Conditions

The engine geometry and the operating conditions for the unsteady-state calculations resemble the data used by Diwakar (1987) from a two-stroke diesel engine of Electro-Motive Division of General Motors. The geometrical and operating conditions are provided in Table 3. The exhaust valve was given an arbitrary motion and the exhaust opening versus crank-angle data defining this motion is shown in Table 4. The corresponding piston motion was calculated from the standard piston velocity formula. The calculations in unsteady situations were started from a point when the exhaust valve just began to open.

Table 3

Geometrical and Operating Condition

Geometry		Operating Conditions	
Bore	0.2302 m	RPM	= 900
Stroke	0.2794 m	Intake manifold	
Con. rod length	0.5842 m	presssure	= 261.04 kPa
Clearance	0.0164 m	Exhaust manifold	
Rvs_{min}	0.033 m	pressure	= 239.04 kPa
Rv_e	0.07 m		
Port	0.0369 m	Intake port angle	
Valve Seat angle	45^o	realtive to radial	= 20^o

Table 4

Exhaust valve opening

Crank angle from tdc	Fraction of exhaust port opening
0.0	0.0
90.0	0.0
104.0	0.0
110.0	0.033
120.0	0.1166
130.0	0.230
140.0	0.393
150.0	0.656
160.0	0.863
170.0	0.979
173.0	1.0
180.0	0.917
190.0	0.77
200.0	0.545
210.0	0.344
220.0	0.182
230.0	0.074
239.5	0.0
300.0	0.0
360.0	0.0

Boundary Conditions

The boundary conditions are incorporated by specification of the dependent variables or associated fluxes or linkages between the two at the enclosing surfaces of the chamber which include the inlet and outlet apertures. The velocity and temperature across the wall layer are described by :

for $Y^+ \leq 11.63$ $\quad U^+ = Y^+$ and $T^+ = Y^+$

for $Y^+ > 11.63$ $\quad U^+ = \frac{1}{k} \log_e(EY^+)$

where $K = 0.4187$ and $E = 9.793$ and

$$T^+ = \delta_{h,T}\left[U^+ + P\left(\frac{\delta_h}{\delta_{h,T}}\right)\right]$$

The function $P\left(\frac{\delta_h}{\delta_{h,T}}\right) = 9.0\left[\frac{\delta_h}{\delta_{h,T}} - 1\right]\left[\frac{\delta_h}{\delta_{h,T}}\right]^{-\frac{1}{4}}$

where δ_h and $\delta_{h,T}$ are laminar and turbulent Prandtl numbers respectively and their values are $\delta_h = 0.7$, $\delta_{h,T} = 0.9$.

The wall shear stress and the dissipation rate within the fully turbulent sub-layer is defined by:

$$\varepsilon = \frac{C_\mu^{\frac{3}{4}} \kappa^{\frac{3}{2}}}{KY} \quad \text{and} \quad \tau_w = \frac{\rho C_\mu^{\frac{1}{4}} \kappa^{\frac{1}{2}} KU}{\log_e(EY^+)}$$

Within the viscous sub-layer, the wall shear stress is given. The turbulent kinetic energy and its dissipation rate for the flow entering through inlet port and the exhaust valve are evaluated from $K_A = 0.01 U_A^2$ and $\varepsilon_A = \left(C_\mu^{\frac{3}{4}} K^{\frac{3}{2}}\right)/1_A$ following the convention. The turbulent length-scale 1_A at inlet port was estimated as 4.5% of the port height while that at the exhaust valve was estimated as 4.5% of the valve gap.
by:

$$\tau_w = \frac{\mu U}{Y}$$

The boundary conditions at the symmetry axis are given by $\frac{\partial\varphi}{\partial r} = 0$ for all the variables except the radial velocity which is itself zero.

The profiles of the axial and radial velocities across the apertures were specified assuming that the flow entered the inlet port or the exhaust valve with a uniform distribution. The equations used for the calculation of mass flow rate are typical of those used in engine cycle calculations and are as follows:
for subsonic flow

$$\dot{m}_A = C_d A_a \rho_u \sqrt{K R_g T_a} \sqrt{\left(\frac{2}{K+1}\right)\left(\frac{P_d}{P_u}\right)\left[1 - \left(\frac{P_d}{P_u}\right)^{\frac{K-1}{K}}\right]}$$

and for sonic flow

$$\dot{m}_A = C_d A_a \rho_u \sqrt{K R_g T_a} \sqrt{\left(\frac{2}{K+1}\right)^{\frac{K+1}{K-1}}}$$

The stagnation enthalpy in the fluid entering through the inlet port and the exhaust valve are given by:

$$h_o = C_p T + \tfrac{1}{2} U_i^2 + \tfrac{1}{2} \overline{U_i U_i}$$

where $\frac{1}{2} U_i^2$ is the kinetic energy of the mean flow

and $\frac{1}{2} \overline{U_i U_i}$ is the turbulent kinetic energy.

The turbulent kinetic energy and its dissipation rate for the flow entering inlet port and the exhaust valve are evaluated from $K_A = 0.01 U_A^2$ and $\varepsilon_A = \frac{C_\mu^{\frac{3}{4}}}{1_A} K_A^{\frac{3}{2}}$ following the convention. The turbulent length-scale 1_A at inlet port was estimated as 4.5% of the port height while that at the exhaust valve was estimated as 4.5% of the valve gap.

Initial Conditions

The program permits specification of the initial conditions arbitrarily as long as they are thermodynamically consistent. In the present situation the initial pressure and temperature in the engine cylinder were provided by specifying the trapped pressure and temperature. This was typically, $P_{trap} = 5.98 \times 10^5$ N/m^2 and $T_{trap} = 1198^\circ$K. During the unsteady calculations the initial concentration of the fresh air in the cylinder was assumed to be zero while the concentration of that of the burnt gas was assigned a value of 1. The initial value of the in-cylinder turbulence kinetic energy was given as 0.5% of the square of mean piston velocity. The initial value of the turbulence length-scale was assumed to 3% of the chamber bore. The initial field values for the density were evaluated from the trapped conditions. The initial value of the dissipation rate of the turbulent kinetic energy was calculated from the specified initial values of turbulent kinetic energy and the turbulence length-scale. The initial field values of viscosity were set to those at standard atmospheric conditions since they affected the calculations very litle. The initial values of all other variables were set to zero.

RESULTS

The predictions include contour plots of velocities in the entire flow-field. Vector diagrams of the flow-field in the radial-axial plane are also drawn so that the existence of any recirculating zone can be easily identified. The above results are obtained for various crank-angle degrees of interest. In addition to these, for obtaining information about the distribution of fresh air and burnt gases in the flow-field, the concentration contours are plotted. The results have been presented in figures 2-10. The crank-angle positions chosen are 149^{o}, 169^{o} and 239^{o} after top dead centre (atdc).

DISCUSSIONS

From the point of view of those concerned with the design and improvement of internal combustion engines, the unsteady-flow solution of the in-cylinder flow problems would be much desirable. The purpose of the present program is a small step towards achieving that goal. The geometrical and operating conditions chosen for the engine correspond to the EMD two-stroke diesel engine of the General Motors Research Laboratory with the bowl shaped piston replaced by a flat-top piston. The running speed wad determined on the basis of the volumetric flow-rate corresponding to a non-supercharged engine rotating at 2000 rpm having a delivery ratio of 1.0. However, in a real engine the scavenging process is allowed about one-third of the total cycle time and the port area varies during that time. Hence it was assumed that to get a better representation of the velocity field, which prevails inside the cylinder, the engine speed should be accordingly reduced. Allowing a factor of 1/3 for the period during which scavenging takes place and a factor of 2/3 for the variation of port area during scavenging, the appropriate value of the engine speed was estimated to be 450 rpm.

The vector plot of figure 2 at 149^{o} CA (crank-angle) is quite straight-forward where the flow occurs due to the pressure difference between the inlet and the exhaust manifolds. The flow comes in through the intake ports establishes a very small recirculation region due to the flow entrainment near the cylinder wall. The flow-field has similarity to that obtained by Diwakar (1987) except that the recirculation near the wall in his case is stronger. The difference might be attributed to some extent to the different means of inlet port modellig between the two solutions. It is worth mentioning that Diwakar modelled the individual inlet ports while in the present program the port was assumed to be a uniform slot on the cylinder circumference. At this position the distribution of the tangential velocity is seen to be limited to the areas closer to the outer radius in the piston end as shown in figure 5.

At 169^{o} CA position the flow-field inside the cylinder clearly shows the presence of two recirculation zones. One recirculation zone is in the lower half of the cylinder near the cylinder wall and the second recirculation is near the axis. The former is seen to have grown from its earlier size in the axial direction due to the upward motion of the fresh charge induced by the axial pressure gradient. The latter extends from about three-quarters of the total cylinder length down to the piston top as shown in figure 3. As far as the peripheral recirculation is concerned there is not much difference between the present results and those of Diwakar but in his case the axial recirculation does not not extend upto the piston top. The reason is obvious. His piston geometry contains a bowl which redirects the flow upward thereby the growth of the recirculation is restricted to the mid-cylinder area. At this crank-angle about three-quarters of the whole cylinder experiences the swirl velocity. The contours of higher tangential velocity are seen to lie in the mid-radius region. The magnitude of the tangential velocities show a decreasing trend in the downstream direction as shown in figure 6.

At 239^{o} CA when both inlet and exhaust valves are closed, the velocity field gets weaker as demonstrated in figure 4. The recirculating flow in the wall area is seen to disappear but the recirculation at the axial region persists. Swirl velocity is seen to spread over the whole of the cylinder volume. The lowest tangential velocities occur near the cylinder axis and the swirl contours rearrange themselves in such a pattern that the higher the radius, the bigger the magnitude of swirl. This is shown in figure 7. However, it should be noted that at the piston end swirl distribution is like that at 169^{o} CA, i.e. higher tangential velocities in the mid-radius region.

Figure 8 shows the contour plot for the concentration of fresh charge at 149^{o} CA shortly after the inlet port has opened. Most of the cylinder is still filled with the exhaust gas. Fresh charge has started to push in and all the fresh charge concentration contours are arranged near the peripheral region close to the inlet port.

At 169^{o} CA when the inlet port is nearly fully open, the region containing the fresh charge has grown in size appreciably. Considering the contour having the largest concentration of fresh charge as the front of fresh air it may be observed that the front has a bulging shape at the middle as shown in figure 9. This indicates that the fresh charge coming through the inlet port moves axially upward pushing the residual gases in front of it. Thus the mid-radius region of the cylinder is well scavenged through about half the cylinder length. The recirculation regions at the axis and near the wall, however, entrain the residual gases thereby producing regions of high concentration of burnt gases in those zones.

At 180^{o} CA the fresh charge front moves further inward and as such the size of the unscavenged core of the residuals is reduced. The region of residual gases near the wall is also seen to shrink. Further down the cylinder, turbulence diffusion and high swirl velocity contaminates the fresh charge as is evident from the location of the contours in figure 10.

CONCLUSIONS

The present program successfully predicts the

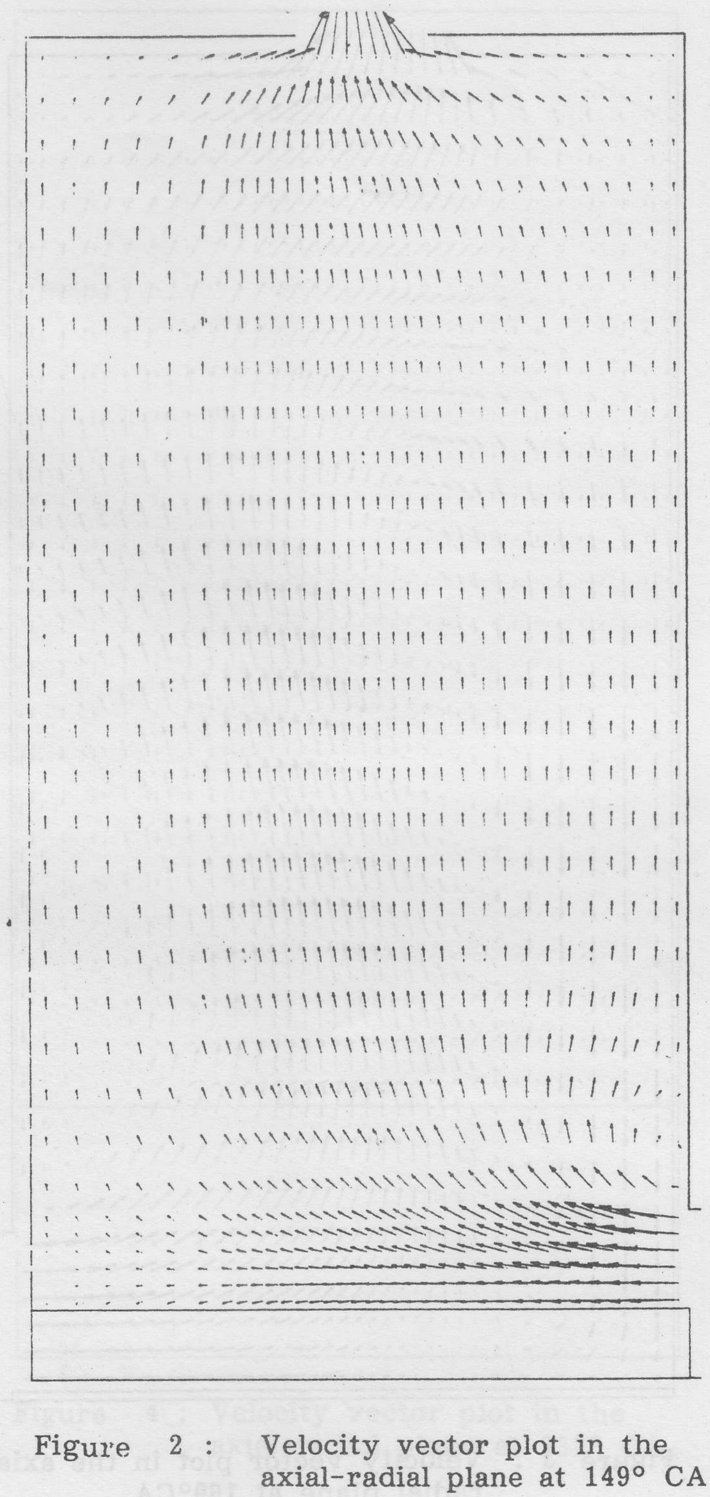

Figure 2 : Velocity vector plot in the axial-radial plane at 149° CA.

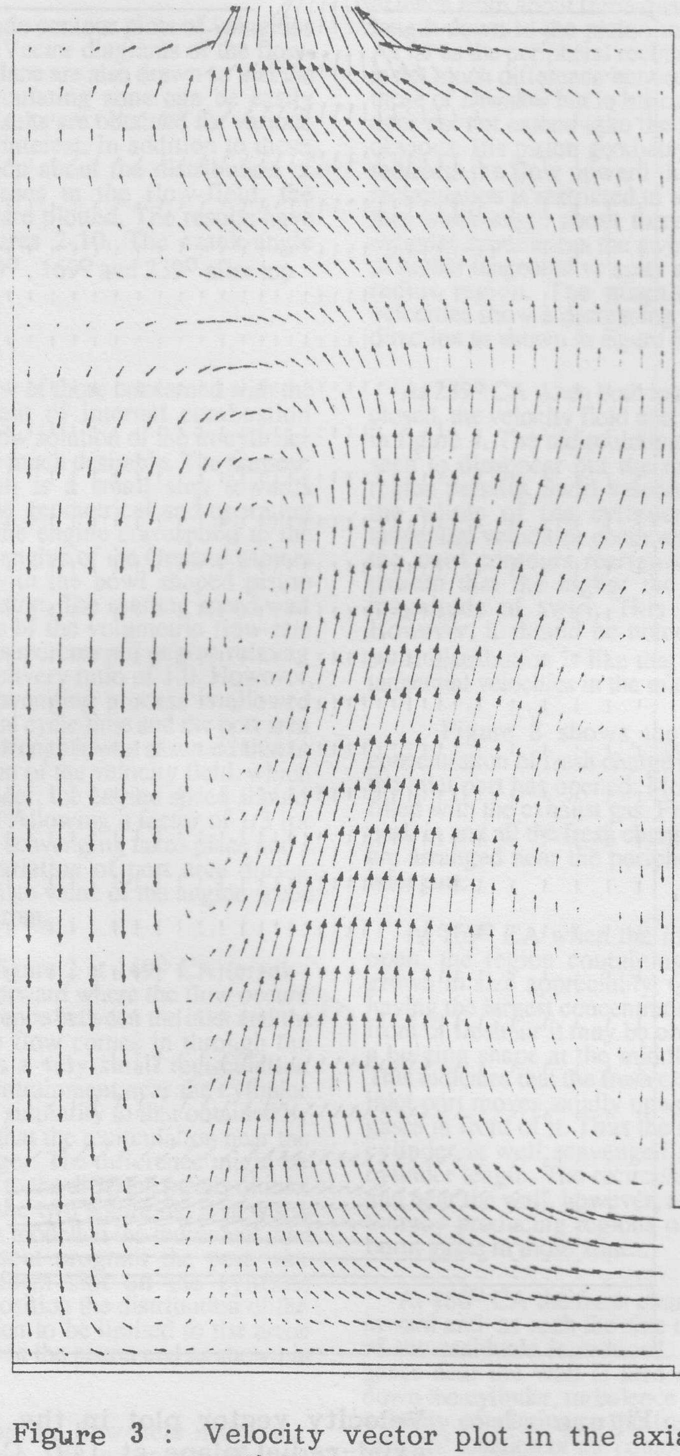

Figure 3 : Velocity vector plot in the axial-radial plane at 169°CA.

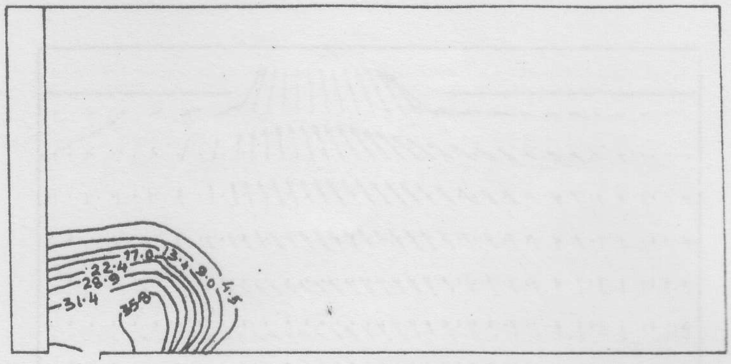

Figure 5 : Contour plot of Tangential mean velocity at 149° CA.

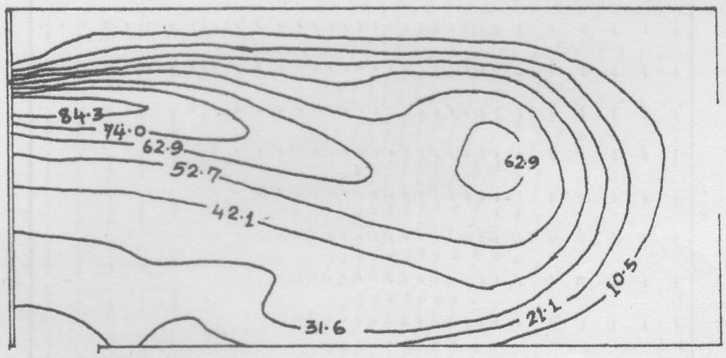

Figure 6 ; Contour plot of Tangential mean velocity at 169° CA.

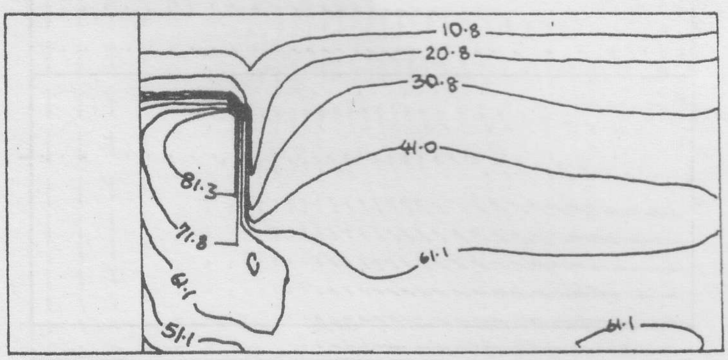

Figure 7 : Contour plot of Tangential mean velocity at 239° CA,

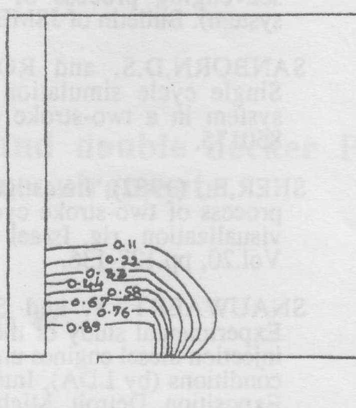

Figure 8 : Contour plot of Concentration of fresh air at 149° CA.

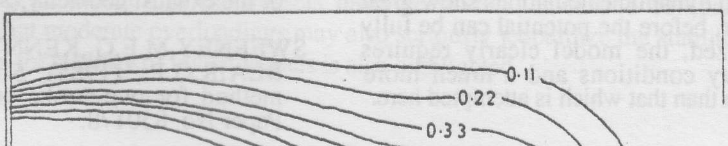

Figure 9 : Contour plot of Concentration of fresh air at 169° CA.

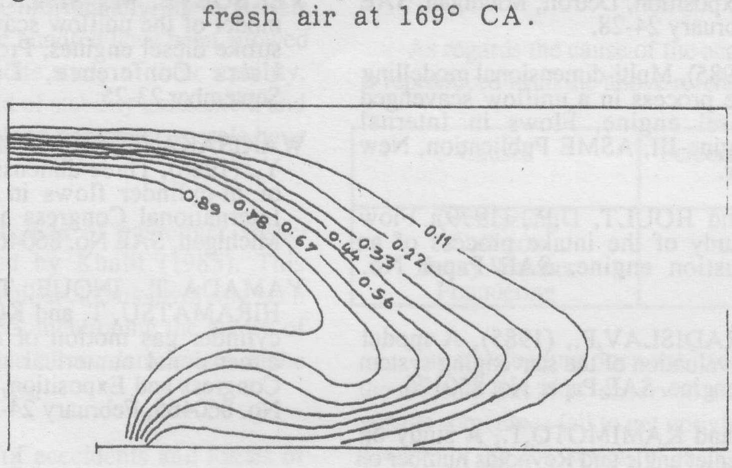

Figure 10: Contour plot of Concentration of fresh air at 180° CA.

unsteady flow-field inside the cylinder of a motored uniflow two-stroke cycle engine. There are, of course, minor differences in the flow structures when compared with results of similar work carried out by other workers. The differences have been explained by the basic physical processes that take place in the two situations. The contribution of the piston movement and boundary conditions in this respect have also been analysed.

The prediction of the concentration distribution by use of the present program is quite satisfactory. The corresponding contour plots have considerable agreement with similar work undertaken by other workers even though certain aspects of the data had to be assumed (e.g. inlet and outlet turbulent quantities, exhaust concentration distribution etc.). In general the predictions showed that the scavenging process is adversely affected by the strong swirl produced inside the cylinder.

As a means of gaining insight into the in-cylinder flow development during scavenging the computational fluid dynamic calculations show great potential. However, before the potential can be fully realized and utilized, the model clearly requires improved boundary conditions and a much more complete validation than that which is attempted here.

REFERENCES :

AMSDEN,A.A.,RAMSHAW,J.D., O'ROURKE,P.J. and DUKOWICZ, J.K. KIVA, (1985), A computer programme for two and three dimensional fluid flows with chemical reactions and fuel spray. Los Alasmos National Lab Report. L. 10245-MS.

DIWAKAR,R., (1987), Three dimwnsional modelling of the in-cylinder gas exchange processes in a uniflow scavenged two-stroke engine, International Congress and Exposition, Detroit, Michigan, SAE No. 860465, February 24-28.

DIWAKAR,R., (1985), Multi-dimensional modelling of gas exchange process in a uniflow scavenged two-stroke diesel engine, Flows in Internal Combustion Engine-III, ASME Publication, New York, November.

ECCHIAN, A. and HOULT, D.P., (1979), Flow visualization study of the intake process of an internal combustion engine. SAE Paper No. 790095.

MIRKO,C. and RADISLAV,P., (1985), A model method for the evaluation of the scavenging system in a two-stroke engine. SAE Paper No. 850176.

NISHIMOTO,K. and KAMIMOTO,T., A study on the influence of inlet angle and Reynolds number on the flow-pattern of uniflow scavenging air.

OHIGASHI,S.,KASHIWADA,Y. and ACHIEWA,J., (1960),, Scavenging the two-stroke diesel engine (effect of inlet port angle on scavenging process of a through scavenging system). Bulletin of JSME,Vol.3,No.9.

SANBORN,D.S. and ROEDER,W.M., (1985), Single cycle simulation simplifies scavenging system in a two-stroke engine.SAE Paper No. 850175.

SHER,E., (1982), Investigating the gas exchange process of two-stroke cycle engine with a flow visualization rig. Israel Journal of Technology, Vol.20, pp.127-136.

SNAUWAERT, P. and SIERENS, R., (1986), Experimental study of the swirl motion in direct injection diesel engines under the steady-state flow conditions (by LDA), International COngress and Exposition, Detroit, Michigan, SAE No. 860026, February 24-18.

SUNG, N.W. and PATTERSON, D.J., (1982), Air motion in a two-stroke engine cylinder - the effects of the exhaust geometry, SAE Paper No. 820751.

SWEENEY,M.E.G.,KENNY,R.B.G.,AND BLAIR,G.P., (1985), Single cycle gas testing method for two-stroke engine scavenging. SAE Paper No. 850178.

TINDAL,M.N., WILLIAMS,T.J., AND EL KHAFAZI, A.H.A., (1974), Gas flow measurements in engine cylinders. National Combined Farm, Construction and Industrial Machinery and Powerplat Meetings, Milwaukee, Wisconsin, No. 740719, September 9-12.

VAFIDIS, C., and WHITELAW, J.H., (1986), Intake valve and in-cyinder flow development in a reciprocating model engine, Proc. I. Mech. Engrs. Vol. 200, No. C2.

VERBOEVE, M., SISCA, (1985), A simulation model of the uniflow scavenging process of two-stroke diesel engines, Proc. Ist Internal Phoenics Users Conference, Dartford, Kent, U.K., September 23-25.

WAKISAKA, T., SHIMAMOTO, Y., and ISSHIKI, Y., (1986), Three-dimensional numerical analysis of in-cylinder flows in reciprocating engines, International Congress and Exposition, Detroit, Michigan, SAE No. 860464, February 24-18.

YAMADA T., INOUE, T., YOSHIMATSU, A., HIRAMATSU, T. and KONISHI, M., (1986), In-cylinder gas motion of multivalve engine-three dimensional numerical simulation, International Congress and Exposition, Detroit, Michigan, SAE No. 860465, February 24-28.

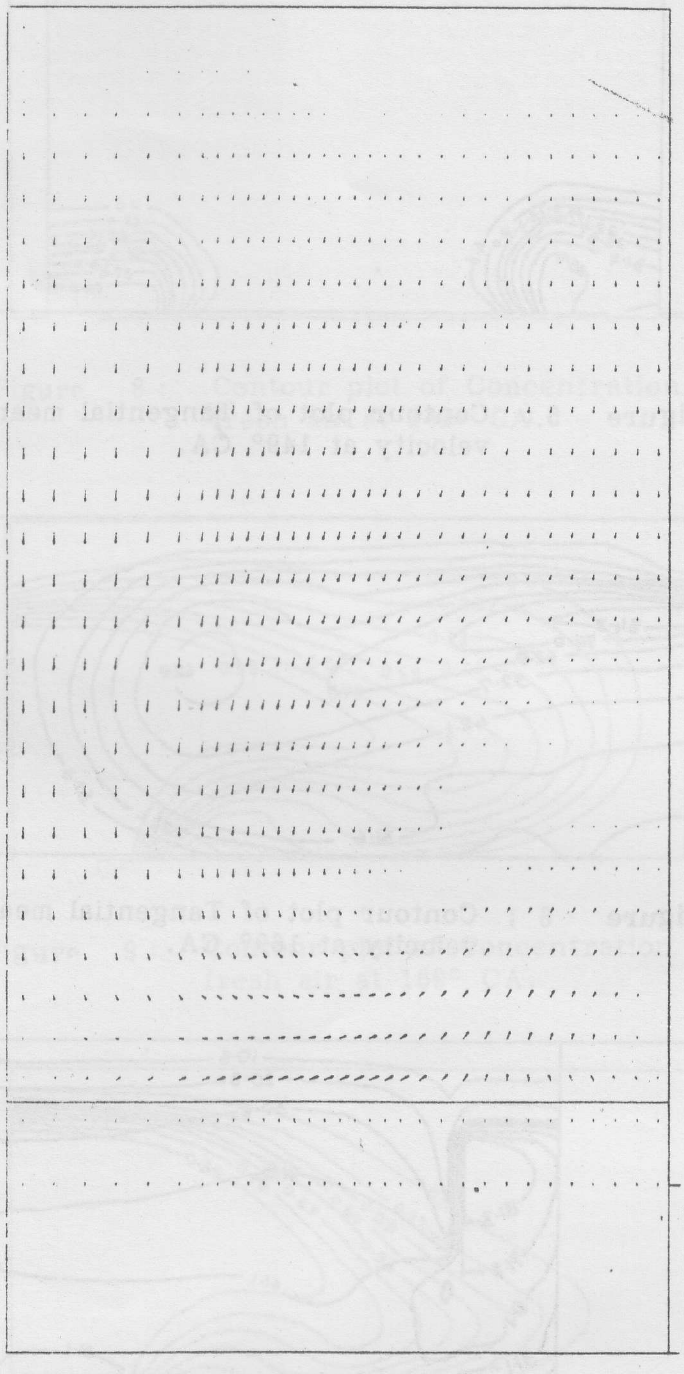

Figure 4 : Velocity vector plot in the axial-radial plane at 239° CA.